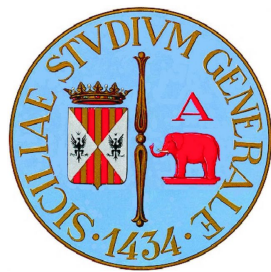


**UNIVERSITÀ DEGLI STUDI DI CATANIA**

---



Dipartimento di Fisica e Astronomia

**Doctor of Philosophy**  
**CYCLE XXXI**  
**Physics**

# **$K^*(892)^\pm$ resonance with ALICE detector at LHC**

**Candidate:**

Kunal GARG

**Coordinator:**

Prof. Francesco Riggi

**Supervisor:**

Dr. Angela Badala

*Some quote here*

# CONTENTS

1	physics of the quark-gluon plasma	1
1.1	Standard Model	1
1.2	Quantum Chromodynamics and Quark-Gluon Plasma	1
1.3	Heavy-Ion Physics	1
1.4	Physics of Small systems	1
2	hadronic resonance production in pp and heavy-ion collisions	2
2.1	Strange hadronic resonance production	2
2.1.1	Strangeness Production	2
2.1.2	Resonances and Chemical and Kinetic freeze-out	2
2.2	Recent resonance results at the LHC	2
2.2.1	Resonances in pp and p-Pb collisions	2
2.2.2	Resonances in Pb-Pb collisions	2
2.3	Theoretical Models	2
2.3.1	Microscopic Models	2
2.3.2	Statistical Models	2
2.3.3	Hybrid Models	3
3	a large ion collider experiment at lhc	4
3.1	The Large Hadron Collider	4
3.1.1	The LHC as a heavy-ion accelerator	5
3.2	The ALICE Detector	7
3.2.1	Inner Tracking System	11
3.2.2	The Time Projection Chamber	13
3.2.3	The Time of Flight Detector	15
3.2.4	VZERO	16
3.2.5	Data Acquisition (DAQ) and Trigger systems	17
3.2.6	Data flow: from the Online to the Offline	19
3.2.7	ALICE Offline software framework	21
3.2.8	Event reconstruction	24
3.2.9	Particle identification with the TPC	25
3.2.10	Centrality Determination?	27
3.2.11	ITS UPGRADE?	27

4	$K^{*0}$ and $K^{*\pm}$ resonance reconstruction in pp collisions	29
4.1	Signal Extraction . . . . .	29
4.1.1	Uncorrelated background estimate . . . . .	29
4.2	$K^{*\pm}$ Mass Determination . . . . .	29
4.2.1	Systematic uncertainty on mass estimation . . . . .	29
5	measurement of $K^{*\pm}$ production in pp collisions	30
5.1	$K^{*\pm}$ reconstruction in pp collisions . . . . .	30
5.1.1	Data sample and event selection . . . . .	30
5.1.2	Primary pion selection . . . . .	30
5.1.3	$V^0$ selection . . . . .	30
5.1.4	Signal Extraction . . . . .	31
5.1.5	Raw Yield Estimation . . . . .	31
5.2	Efficiency Correction . . . . .	31
5.3	Systematic Uncertainties estimation . . . . .	31
5.4	$K^{*\pm}$ transverse momentum spectrum . . . . .	31
6	$k^0$ comparisons	32
6.1	$K^0$ reconstruction in pp collisions . . . . .	32
6.2	Comparison of $K^0$ and $K^{*\pm}$ . . . . .	32
7	further results and discussions	33
7.1	Particle Ratios . . . . .	33
7.2	Model Comparison . . . . .	33
7.3	Energy Dependence . . . . .	33
7.4	$K^{*+}$ vs $K^{*-}$ . . . . .	33
	<b>Conclusions</b>	34

## LIST OF FIGURES

Figure 1	The CERN accelerator complex.	6
Figure 2	The ALICE detector	8
Figure 3	Cross Section of Central Barrel of ALICE	9
Figure 4	Inner Tracking System	12
Figure 5	dE/dx distribution of charged particles as function of their momentum, both measured by the ITS alone, in pp collisions at 13 TeV. The lines are a parametrization of the detector response based on the Bethe-Bloch formula.	14
Figure 6	Momentum resolution for TPC-ITS	15
Figure 7	Energy loss in TPC in pp collisions at $\sqrt{s} = 13\text{TeV}$	16
Figure 8	TOF $\beta$ vs $p_T$ performance plot in pp collisions at $\sqrt{s} = 13\text{TeV}$	17
Figure 9	ALICE DAQ system	19
Figure 10	ALICE Data Flow	20
Figure 11	ALICE Grid sites	22
Figure 12	AliRoot framework	23
Figure 13	ALICE track reconstruction principle	28

## LIST OF TABLES

# 1

## PHYSICS OF THE QUARK-GLUON PLASMA

### **1.1 Standard Model**

Short description of the standard model of elementary particle physics

### **1.2 Quantum Chromodynamics and Quark-Gluon Plasma**

Here we describe the theory of QCD and the physics of Quark Gluon Plasma

### **1.3 Heavy-Ion Physics**

Heavy-ion collisions is the realm where we can probe the properties of the quark gluon plasma

### **1.4 Physics of Small systems**

The physics in pp collisions is important for nuclear physics to set a baseline for the heavy-ion physics

# 2 | HADRONIC RESONANCE PRODUCTION IN PP AND HEAVY-ION COLLISIONS

## **2.1 Strange hadronic resonance production**

Strange hadronic resonances are important since net strangeness content of initial colliding system is zero.

2.1.1 Strangeness Production

2.1.2 Resonances and Chemical and Kinetic freeze-out

## **2.2 Recent resonance results at the LHC**

2.2.1 Resonances in pp and p-Pb collisions

2.2.2 Resonances in Pb-Pb collisions

## **2.3 Theoretical Models**

Here we discuss the different theoretical models which explain the dynamics of the colliding systems

2.3.1 Microscopic Models

eg.. PYTHIA

2.3.2 Statistical Models

Will be included based on the decision of whether to do Pb-Pb analysis or not.

### 2.3.3 Hybrid Models

eg. EPOS

# 3 | A LARGE ION COLLIDER EXPERIMENT AT LHC

## 3.1 The Large Hadron Collider

The Large Hadron Collider (LHC) is the world's largest and most powerful particle accelerator. It was inaugurated on 10 September 2008, and consists of a 27-kilometre ring of superconducting magnets with a number of accelerating structures to boost the energy of the particles along the way. By design, the maximum energies reached in the accelerator are 7 TeV for a beam of protons and 2.76 TeV per nucleon for a beam of lead ions, thus providing collisions at  $\sqrt{s} = 14$  TeV and  $\sqrt{s_{NN}} = 5.5$  TeV, respectively. During Run 2, LHC was able to reach 13 TeV for pp and 2.51 TeV for Pb-Pb collisions. These are the largest energies ever achieved in particle collision experiments.

Inside the accelerator, two high-energy particle beams travel at close to the speed of light before they are made to collide. The beams travel in opposite directions in separate beam pipes - two tubes kept at ultrahigh vacuum. They are guided around the accelerator ring by a strong magnetic field maintained by superconducting electromagnets. The accelerator bends the beams around the ring, keeping the bunches focused and accelerate them to their collision energy. Finally, bunches are squeezed in order to ensure a high number of collisions per time interval at the collision points, i.e. a high luminosity<sup>1</sup>. A combination of magnetic and electric fields components perform the mentioned tasks. Despite the high luminosity reached, only a very small fraction of the particles from the two bunches collide in a single bunch crossing. The others leave the interaction region essentially uninfluenced, and continue to circulate in the accelerator.

---

<sup>1</sup> For a particle accelerator experiment, the luminosity is defined by:  $\mathcal{L} = fnN^2/A$  with  $n$  number of bunches in both beams,  $N$  number of particles per bunch, cross-sectional area  $A$  of the beams that overlap completely, and revolution frequency  $f$ . The frequency of interactions (or in general of a given process) can be calculated from the corresponding cross-section  $\sigma$  and the luminosity:  $dN/dt = \mathcal{L}\sigma$ .

Injection of bunches into the LHC (Figure 1) is preceded by acceleration in the LINAC<sub>2</sub>, PS booster, PS, and SPS accelerators. The acceleration sequence is slightly different for heavy-ions, in which case bunches pass the LINAC<sub>3</sub>, LEIR, PS, and SPS accelerators. Several injections to the LHC are needed until all bunches of both beams are filled. The LHC produces collisions in four so called Interaction Points (IPs) in correspondence of which are located six detectors of different dimensions and with different goals, all able to study the products of the interactions. These are:

- **ALICE (A Large Ion Collider Experiment - IP2):** is a dedicated heavy-ion experiment designed to study strongly-interacting matter at very high energy density. A detailed description of ALICE detector will be covered in the next section.
- **ATLAS (A Toroidal LHC ApparatuS - IP1) and CMS (Compact Muon Solenoid - IP5):** are general-purpose detectors for pp collisions that are built to search for the Higgs boson and physics beyond the Standard Model, e.g. new heavy particles postulated by supersymmetric extensions (SUSY) of the Standard Model and evidence of extra dimensions. They have discovered the Higgs boson in 2012.
- **LHCb (The Large Hadron Collider beauty experiment - IP8):** is a dedicated experiment to study heavy flavour physics at the LHC. The experiment complements the studies conducted at B-factories and the search for new particles at ATLAS and CMS.
- **LHCf (Large Hadron Collider forward experiment - IP1):** is placed closed to the ATLAS experiment and studies the forward particles created during LHC collisions.
- **TOTEM (TOTal Elastic and diffractive cross-section Measurement - IP5):** is located close to the CMS detector and measures the total cross-section, elastic scattering, and diffractive processes.

### 3.1.1 The LHC as a heavy-ion accelerator

**OPTIONAL SECTION** Since its early stages, LHC was designed to perform as well as heavy ion collider, in particular to feed ALICE with data, although

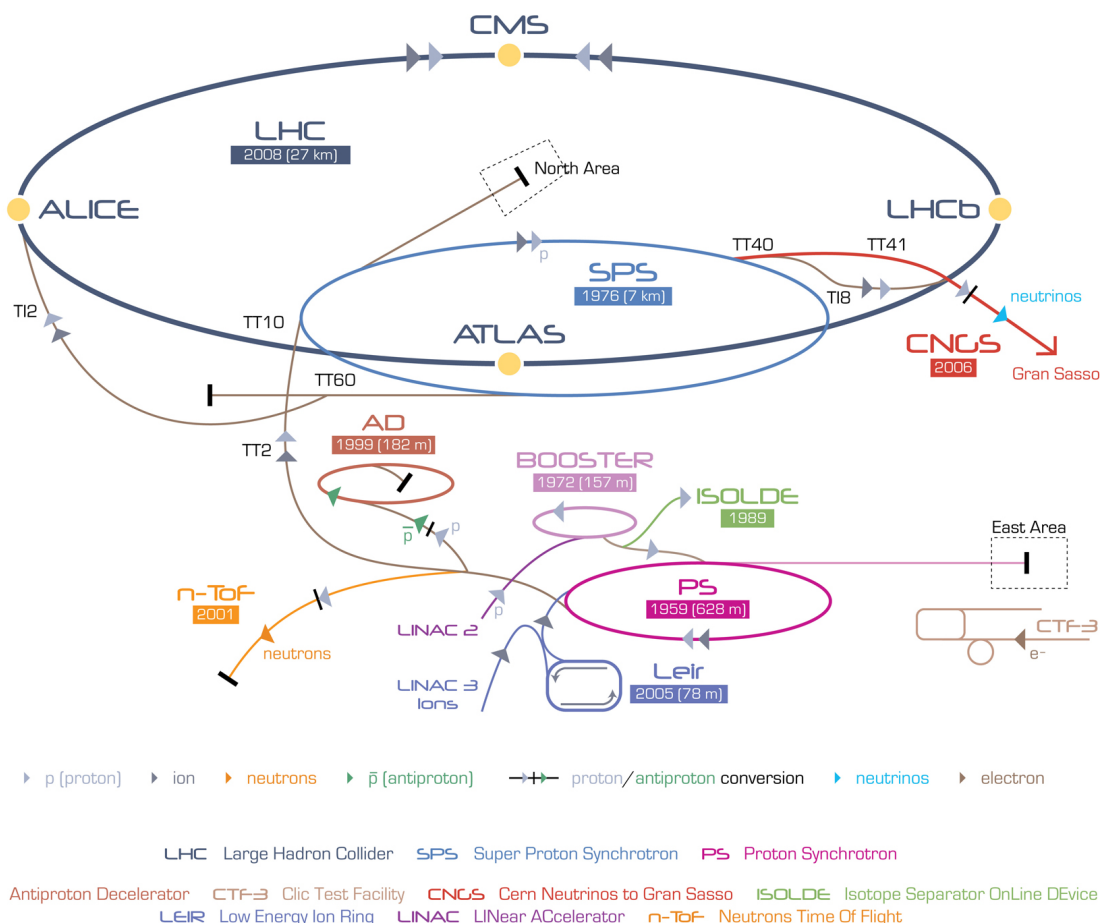


Figure 1: The CERN accelerator complex.

also CMS and ATLAS included the study of ion collisions with similar luminosities in their physics program.<sup>2</sup>

The source of Pb ions is a 3 cm lead cylinder heated to about 500 °C. This vaporises a small amount of atoms, that once partially ionised by strong electrical fields are accelerated in a linear device to strip the remaining electrons to create  $^{208}\text{Pb}^{82+}$  ions. These ions are then injected and accumulated in Low Energy Ion Ring (LEIR) and then sent to the Proton Synchrotron (PS). Further on, they follow the same injection procedure as protons. The ions can reach a centre of mass energy of 5.5 TeV/nucleon or a total centre of mass energy of 1.15 PeV with the nominal magnetic field of 8.33 T in the dipole magnets.

<sup>2</sup> LHCb did not participate in the Pb-Pb run in 2010 and 2011.

### 3.2 The ALICE Detector

ALICE (A Large Ion Collider Experiment) is a general-purpose, heavy-ion detector at the LHC which focuses on Quantum Chromodynamics, the strong-interaction sector of the Standard Model. It has been collecting data since the beginning of LHC operations in 2008 and will continue to do so until the end of 2018 for the planned long shutdown. During the first three years of operations LHC provided pp collisions at 0.9, 2.76, 7 and 8 TeV, Pb-Pb collisions at 2.76 TeV and finally p-Pb collisions at 5.02 TeV and in the second phase, LHC reached close to its designed maximum energies at 13 TeV for pp, and 5.02 TeV for Pb-Pb and 8 TeV at p-Pb collisions. It has been designed to study the physics of strongly interacting matter and the quark-gluon plasma at extreme values of energy density and temperature in nucleus-nucleus collisions. ALICE allows for a comprehensive study of hadrons, electrons, muons, and photons produced in the collision of heavy nuclei (Pb-Pb), up to the highest multiplicities at the LHC. The physics programme also includes analysing proton-proton and proton-nucleus collisions to address various QCD topics. The detector, located at the interaction point 2 along the LHC ring, has been designed to cope with a high particle multiplicity environment and to provide unique particle identification (PID) performance that allow a comprehensive study of hadrons, electrons, muons, and photons produced in the collision, down to very low transverse momentum ( $0.1 \text{ GeV}/c$ ). Figure 2 shows the ALICE detector schema and Figure 3 shows the cross section of the central barrel. The central barrel covers a mid rapidity region  $|\eta| < 0.9$  and azimuthal range of  $2\pi$ .

The central barrel of the detector is enclosed in L3 solenoid magnet which provides a 0.5 T magnetic field, and is followed by a forward muon spectrometer which has its own dipole magnet providing a field of 0.67 T. The central barrel consists of, going from beam pipe outwards, a six layer Inner Tracking System (ITS) that provides precise tracking and vertex reconstruction, a large volume Time Projection Chamber (TPC) which is responsible for global tracking and particle identification (PID) through the measurement of specific energy loss in a gas, a Transition Radiation Detector (TRD) allowing for identification of electrons and the outermost of the central barrel is a Time of Flight detector (TOF) which allows for identification of charged hadrons.

TRD covers full azimuth of the mid-rapidity region ( $-0.84 < \eta < 0.84$ ) from 2.90 m to 3.68 m from the interaction vertex. It has the main task to provide electron identification in the ALICE central barrel for particle momenta greater than  $1 \text{ GeV}/c$ . Electrons with momentum above this value radiate transition radiation

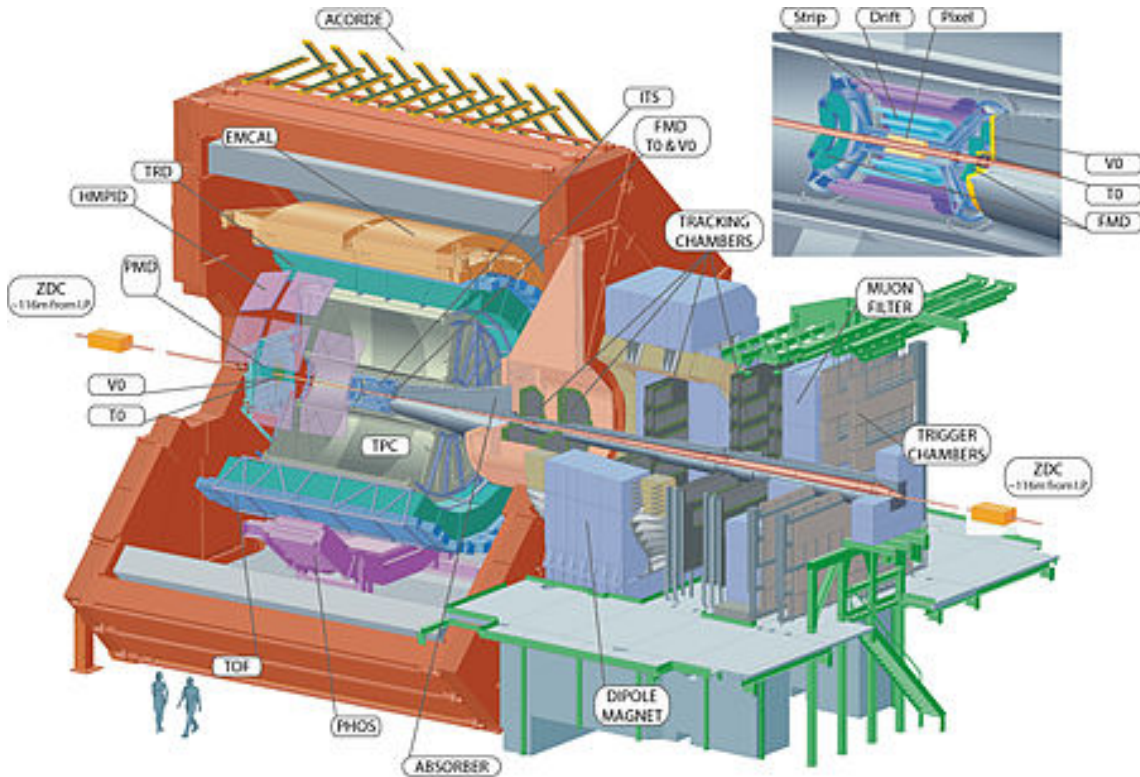


Figure 2: The ALICE detector

<sup>3</sup> which can be exploited to extend the pion rejection capability of the TPC to higher momenta. Furthermore, the TRD provides tracking information with a larger tracking lever arm, thus improving momentum resolution at high  $p_T$ . The detector can also derive a fast trigger for high-momentum charged particles and it contributes to the Level-1 trigger of ALICE.

The detectors which are important to this work will be explained in the following sections (namely TPC, ITS, TOF and VZERO)

---

<sup>3</sup> Transition radiation is produced by relativistic charged particles ( $\gamma \geq 1000$ ) when they cross the interface of two media of different dielectric constant. Photons are emitted in the keV range with typical energy

$$\hbar\omega \approx \frac{1}{4}\hbar\omega_p\gamma,$$

where  $\omega_p$  is the plasma frequency

$$\omega_p = \sqrt{\frac{n_e e^2}{\epsilon_0 m_e}}$$

where  $n_e$  is the electron density

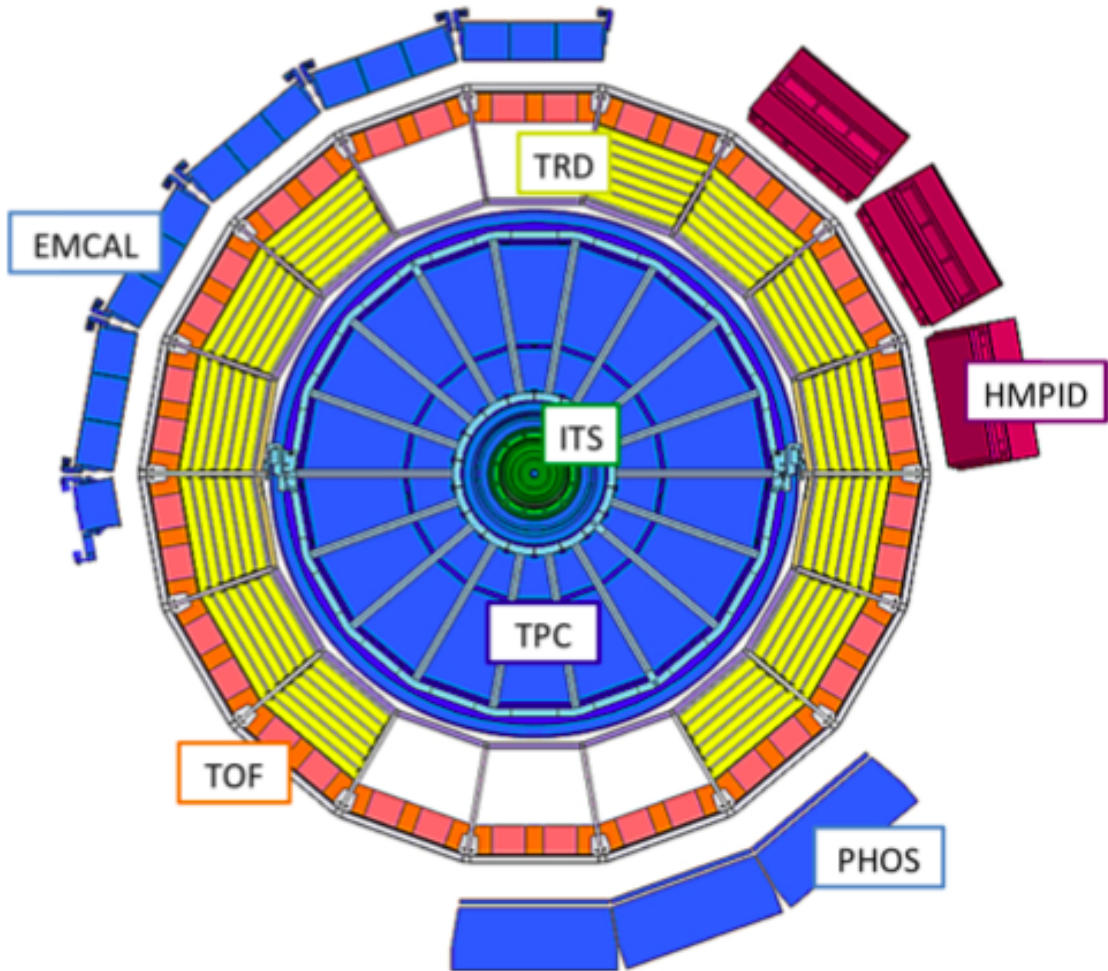


Figure 3: Cross Section of Central Barrel of ALICE

Besides the aforementioned detectors, the following detectors located inside the L<sub>3</sub> magnet provide limited acceptance, outside the TOF:

- **HMPID:** High Momentum Particle Identification detector is a dedicated detector for inclusive measurements of identified hadrons at  $p_T > 1$  GeV/c. It is based on proximity-focusing Ring Imaging Cherenkov (RICH) counters <sup>4</sup> arranged in an array with an acceptance of 5% of the central barrel

---

<sup>4</sup> Cherenkov radiation is emitted when a charged particle passes a dielectric medium with velocity

$$\beta \geq \beta_{\text{thr}} = 1/n$$

phase space with the aim of enhancing the PID capability of ALICE by enabling identification of charged hadrons beyond the momentum interval attainable through energy-loss (in ITS and TPC) and time-of-flight measurements (in TOF). Identification of light nuclei and anti-nuclei ( $d$ ,  $t$ ,  ${}^3\text{He}$ ,  $\alpha$ ) at high transverse momenta in the central rapidity region can also be performed with the HMPID.

### – Calorimeters

1. **EMCal/DCal:** The aim of ElectroMagnetic Calorimeter and Di-Jet Calorimeter is to enable ALICE to measure jet properties and providing trigger on jets and high momentum photons and electrons. The EMCal and DCal are large Pb-scintillator sampling calorimeters with cylindrical geometry, located adjacent to the ALICE magnet coil at a radius of  $\sim 4.5$  metres from the beam line. EMCal subtends  $110^\circ$  and the DCal subtends  $60^\circ$  in  $\phi$ , with both detectors covering  $|\eta| < 0.7$ , thereby providing good acceptance for di-jets with  $R \leq 0.4$  up to transverse momenta  $p_T \sim 150\text{GeV}/c$
2. **PHOS:** Photon Spectrometer is a high-resolution electromagnetic calorimeter which detects electromagnetic particles in a limited acceptance region at central rapidity to provide photon identification as well as neutral-meson reconstruction through the 2-photon decay channel. Its main physics objectives are the test of thermal and dynamical properties of the initial phase of the collision extracted from low  $p_T$  direct photon measurements and the study of jet quenching through the measurement of high- $p_T\pi^0$  and  $\gamma$ -jet correlations. It is positioned at a distance of 460 cm from the interaction point, azimuthally opposed to the EMCAL, and covers a limited acceptance ( $|\eta| < 0.12$  and  $\Delta\phi = 100^\circ$  ).

In addition to the central barrel detectors described above, ALICE has a dedicated Muon Spectrometer, a set of forward detectors and ACORDE.

---

, where  $n$  is the refractive index of the medium. The photons are emitted at an angle

$$\cos\theta_c = \frac{1}{n\beta}$$

### Muon Spectrometer

This detector, placed in the forward pseudo-rapidity region ( $-4.0 < \eta < -2.5$ ), consists of a dipole magnet and tracking and trigger chambers. It is optimised to reconstruct heavy quark resonances (such as  $J/\Psi$  through their  $\mu^+ \mu^-$  decay channel) and single muons

### Forward Detectors

They are placed in the high pseudo-rapidity region (small angles with respect to the beam pipe) they are small and specialised detector systems used for triggering or to measure global event characteristics.

- Time Zero (T0) to measure the event time with precision of the order of tens of picoseconds, as needed by TOF
- VZERO to reject the beam-gas background and to trigger minimum bias events
- Forward Multiplicity Detector (FMD) to provide multiplicity information over a large fraction of the solid angle ( $-3.4 < \eta < -1.7$  and  $1.7 < \eta < 5$ )
- Photon Multiplicity Detector (PMD) to measure the multiplicity and the spatial distribution of photons on an event-by-event basis in the  $2.3 < \eta < 3.7$  region
- Zero Degree Calorimeter (ZDC) to measure and trigger on the impact parameter. The ZDC consists of two calorimeters, one for neutrons (ZDC:ZN) and one for protons (ZDC:ZP), and includes also an electromagnetic calorimeter (ZEM).

### ACORDE

ACORDE is an array of scintillators installed on top of the L3 magnet to trigger on cosmic rays.

#### 3.2.1 Inner Tracking System

ITS is the main detector responsible for measuring the primary vertex of the collisions being the innermost tracking detector closest to the beam pipe. It has

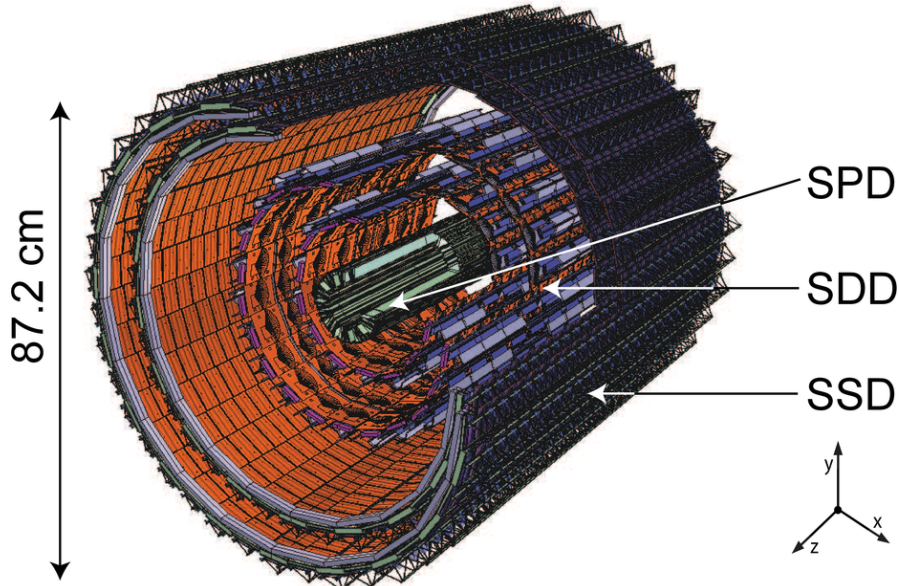


Figure 4: The Inner Tracking System of ALICE

6 layers of concentric cylindrical detectors based on three different technologies of silicon detectors : pixels, drifts and strips (Figure 4). It is positioned at radius between 4 and 43 cm, surrounding the LHC beryllium beam pipe that is 800 $\mu$ m thick and has a radius of 2.9 cm.

The two innermost ITS layers constitute the SPD, Silicon Pixel Detector. A total of  $9.8 \times 10^6$  readout channels receive signals from the 20 half-staves of the SPD, each of them consisting of 240 modules with 1200 readout chips. Thanks to the high-granularity the SPD has also been used for the trigger system, especially for the minimum bias event selection. The SPD is mainly used to determine the primary vertex position, with a resolution of the order of 100 $\mu$ m.

The Silicon Drift Detector (SDD) is based on modules with a sensitive area of  $70.17 (r\phi) \times 75.26 (z)$  mm<sup>2</sup>, divided into two drift regions where electrons move in opposite directions under a drift field of approximately 500 V/cm. The SDD modules are mounted on a linear structure called ladder. The SDD inner layer is made of 14 ladders with 6 modules each, the outer layer has 22 ladders, each of them with 8 modules. The position of the particle along z is reconstructed from the centroid of the collected charge along the anodes, while the position along the drift r coordinate is obtained from the measured drift time with respect to

the trigger time. This reconstruction requires a precise knowledge of the drift speed, that is measured during frequent calibration runs, given its strong dependence from the humidity and temperature gradients in the SDD volume.

The Silicon Strip Detector (SSD) building block is a module composed of one double-sided strip detector connected to two hybrids hosting the front-end electronics. The sensors are  $300\text{ }\mu\text{m}$  thick and with an active area of  $73\text{ (r)} \times 40\text{ (z)}$   $\text{mm}^2$ . There are 768 strips, with a pitch of  $95\text{ }\mu\text{m}$  on each side, almost parallel to the  $z$  beam axis direction. The innermost SSD layer consists of 34 ladders, each of them housing 22 modules along the beam direction, while the other SSD layer has 38 layers, each of them with 25 modules. The outer four layers are used particle identification via energy loss ( $dE/dx$ ) measurement in the non-relativistic region for low momentum particles (down to  $p_T = 100\text{ MeV}$ ) via analogue read-out. Figure 5 shows an example of the particle identification capabilities of the ITS for pp collisions at  $B = 0.2\text{ T}$ . The resolution in the  $r\phi$  plane is nearly  $50\text{ }\mu\text{m}$  for  $1\text{ GeV}/c$  particles and decreases at higher momentum. Resolution in Pb-Pb collisions is slightly better with respect to pp, as the high multiplicity of central Pb-Pb collisions implies a better primary vertex resolution.

## MATERIAL BUDGET REDUCTION AND IMPACT PARAMETER RESOLUTION FOR CHARM RECON

### 3.2.2 The Time Projection Chamber

The Time Projection Chamber (TPC) is the main tracking detector of ALICE covering the pseudorapidity range  $|\eta| < 0.9$  and the full azimuth angle. The optimisation of the detector design has been done to provide excellent tracking performance in a high multiplicity environment, to keep the material budget as low as possible in order to have low multiple scattering and secondary particle production, to limit the detector occupancy at the inner radius but still guarantee a good momentum resolution for high- $\text{p}_T$  particles. TPC is cylindrical in shape 500 cm long along the beam pipe, with 80 cm and 250 cm inner and outer radii respectively, determined by maximum acceptable track density and minimum track length for which the resolution on  $dE/dx$  is lower than 10%. The TPC volume was filled with  $90\text{ m}^3$  of a mixture of Ne/CO<sub>2</sub>/N<sub>2</sub> during Run 1, optimised for drift velocity, low electron diffusion and low radiation length. Neon was replaced by Argon for the second run. The electron drift velocity of  $2.7\text{ cm/s}$  over 250 cm (each of the two TPC drift region separated by the central cathode) gives a maximum drift time of  $88\text{ }\mu\text{s}$ , therefore limiting the maximum

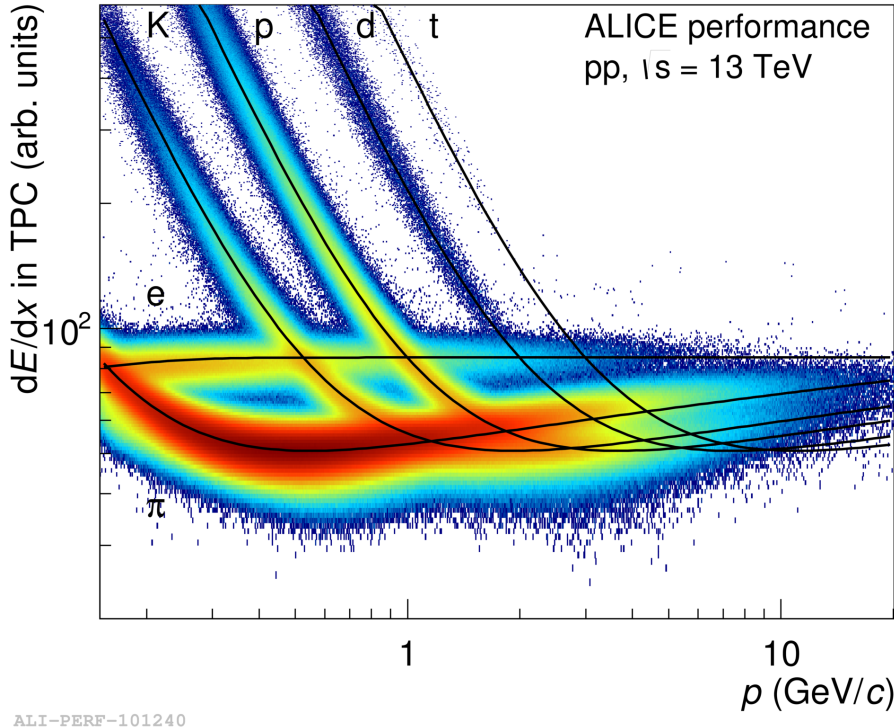


Figure 5:  $dE/dx$  distribution of charged particles as function of their momentum, both measured by the ITS alone, in  $pp$  collisions at 13 TeV. The lines are a parametrization of the detector response based on the Bethe-Bloch formula.

event rate TPC can sustain. At high interaction rate, pile-up effects and the long TPC dead time are the two main factors that force ALICE to run at a lower instantaneous luminosity with respect to the other LHC experiments.

The TPC is able to track particles in a wide momentum range, from about  $p_T \sim 0.1$  GeV/c up to  $p_T \sim 100$  GeV/c with good momentum resolution and efficiency  $> 90\%$  for  $p_T > 100$  MeV/c, where the limiting factor are the interactions in the ITS material. The ITS and the TPC are able to determine the momentum of the charged particles with a resolution better than 1% at low  $p_T$  and better than 20% for  $p_T \sim 100$  GeV/c (see Figure 6) by measuring the deflection in the magnetic field.

The charge collected in the TPC readout pads is used to measure particle energy loss. The momentum measurement and the  $dE/dx$  information allow to separate the various charged particle species in the low momentum region:

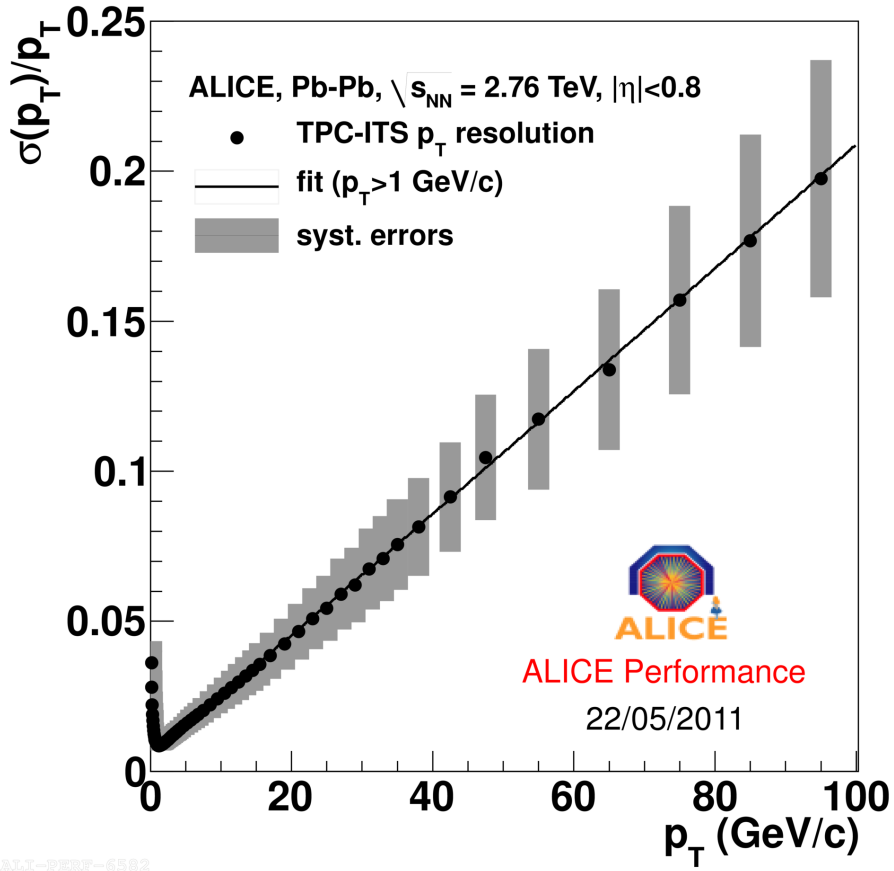


Figure 6: Momentum Resolution for TPC-ITS

thanks to its good  $dE/dx$  resolution, the TPC can identify particles with  $p_T < 1 \text{ GeV}/c$ . An example of the TPC PID performance is shown in Figure 7, where the energy loss distribution for the different species is fitted by a Bethe-Bloch function, similarly to the ITS case.

### 3.2.3 The Time of Flight Detector

TOF plays a key role in particle identification in the pseudorapidity region  $|\eta| < 0.9$ , by combining the measurement of the particle time-of-flight with the momentum information provided by the TPC. TOF is a large MRPC (Multi Resistive Plate Chamber) array located in the ALICE central barrel at a distance of 3.7 m from the beam line, externally to the TRD. The intrinsic time resolution of the MRPC is lower than 50 ps (from test beam studies) and it is dominated by the jitter in the electronics and the time resolution of the TDCs. The MRPC

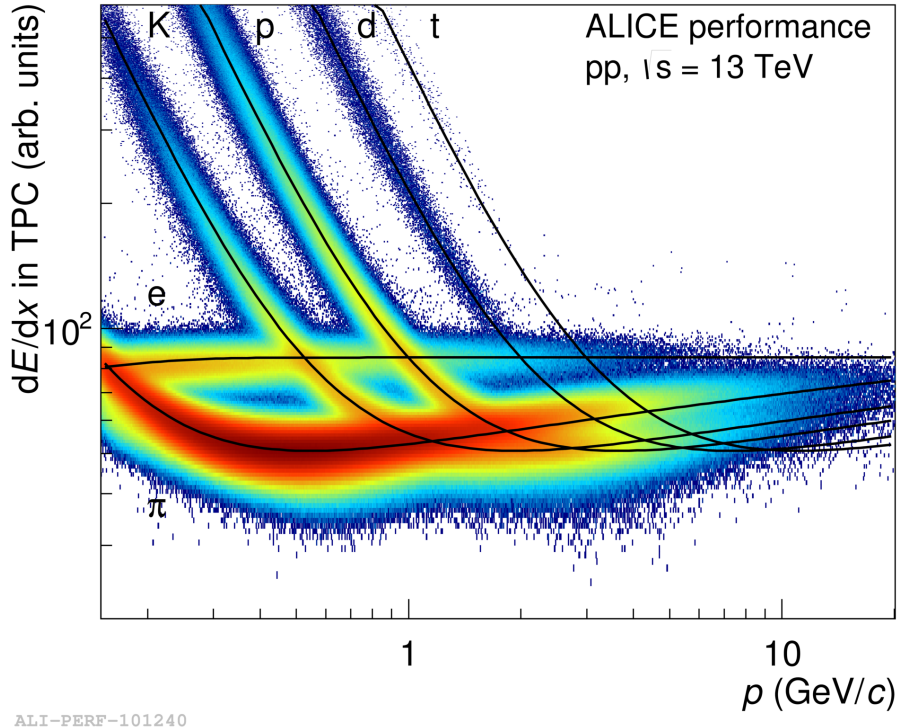


Figure 7: Energy loss in TPC in pp collisions at  $\sqrt{s} = 13\text{TeV}$

efficiency was measured to be close to 100%. The design of TOF is optimised to minimise the dead zones and to be perpendicular to the trajectories of the particles coming from the IP, so to limit the occupancy and reduce the time resolution. The TOF detector consists of 152928 readout channels ( $2.5 \times 3.5 \text{ cm}^2$  each) covering a total area of  $141 \text{ m}^2$ . This highly segmented structure allow to have a low occupancy and good performance also in a high multiplicity environment, such that of  $\text{Pb}\bar{\text{A}}\text{SPb}$  collisions. An example of TOF performance is shown in Figure 8.

### 3.2.4 VZERO

The VZERO is a trigger detector that provides a minimum-bias trigger for all colliding systems to the central barrel detectors and three centrality triggers in  $\text{Pb}\bar{\text{A}}\text{SPb}$  collisions (multiplicity, central and semi-central). It has an important role in rejecting background from beam-gas collisions exploiting the relative time-of-flight measurement between the two arrays: when the beam-gas collision takes place outside the region between the two arrays, particles arrive 6 ns

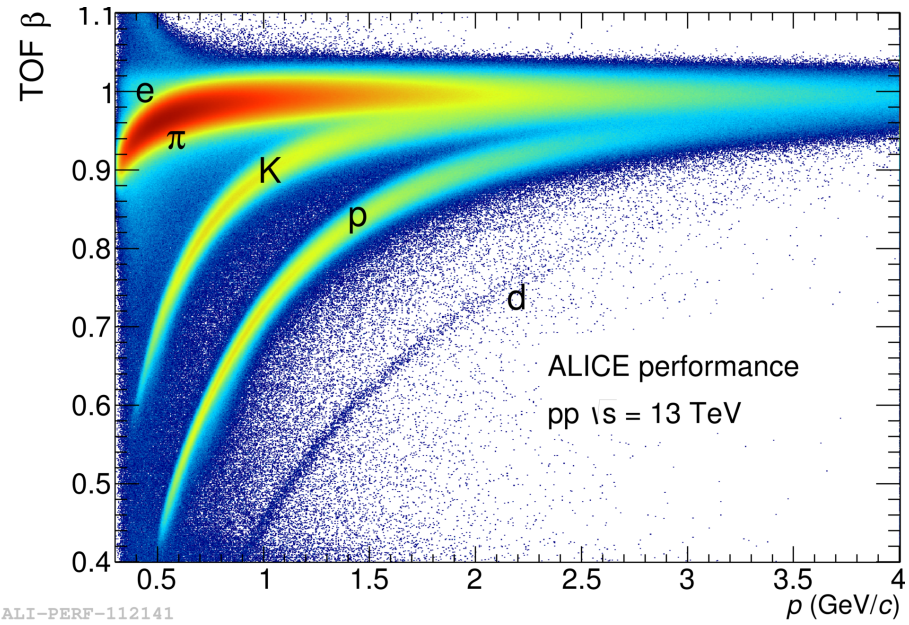


Figure 8: TOF  $\beta$  vs  $p_T$  performance plot in pp collisions at  $\sqrt{s} = 13\text{TeV}$

before or after the time of a beam-beam collision. It consists of two segmented arrays of plastic scintillator counters, called VZERO-A and VZERO-C, placed around the beam-pipe on either side of the IP: one at  $z = 340\text{ cm}$ , covering the pseudo-rapidity range,  $2.8 < \eta < 5.1$ , and the other at  $z = -90\text{ cm}$  (in front of the absorber), covering the pseudo-rapidity range,  $-3.7 < \eta < -1.7$

### 3.2.5 Data Acquisition (DAQ) and Trigger systems

#### Trigger System

The ALICE Central Trigger Processor (CTP) has been designed to select events having a variety of different features at rates which can be scaled down to suit physics requirements and restrictions imposed by the bandwidth of the Data Acquisition (DAQ) system and the High-Level Trigger (HLT). Since the counting rates for different running modes (pp, pA, AA) can vary for almost two orders of magnitude, the biggest challenge for the ALICE trigger is to make optimum use of the detectors and to perform trigger selections in an optimised way for these different modes.

The first response of the trigger system has to be fast to suit detector requirements. The “fast” part of the trigger is split into two levels: a Level-0 (Lo)

signal from CTP reaching the detectors after 1.2  $\mu\text{s}$  and a Level-1 (L1) signal arriving after 6.5  $\mu\text{s}$ . The Lo signal is too fast to enable the trigger inputs from all the detectors while the L1 signal can pick up all the remaining fast inputs. CTP decisions are made in 100 ns.

### Data Acquisition (DAQ)

The trigger and Data Acquisition (DAQ) systems of ALICE have been designed to give different observables a fair share of the trigger and DAQ resources with respect to DAQ bandwidth. They have also to balance the capacity to record Pb-Pb central collisions (which generate large events) with the ability to acquire large fractions of rare events. To provide adequate physics statistics it has been estimated that a bandwidth of 1.25 GB/s to mass storage is suitable. This bandwidth is consistent with constraints imposed by technology, cost and storage capacity.

The architecture of the data acquisition is shown in Figure 9. Detectors receive the trigger signals from CTP (Central Trigger Processor) through LTU (Local Trigger Unit). The data produced by the detectors are injected on the DDL (Detector Data Link) using the same protocol. At the receiving end of the DDL, D-RORC (DAQ Readout Receiver Card) PCI-X based cards receive and assemble the event fragments into sub-events in the LDCs (Local Data Concentrators). The role of the LDC is to ship the sub-events to a farm of machines (Global Data Concentrator, GDC) where the whole events are built. The GDCs feed the recording system which eventually records the events in the Permanent Data Storage (PDS).

### High Level Trigger (HLT)

According to the simulation studies, the amount of data produced in the TPC alone, in a single central nucleus-nucleus collision, corresponds to about 75 MB assuming  $dN_{\text{ch}}/d\eta = 8000$  at mid-rapidity. The data rate for all detectors, resulting after a trigger selection, can easily reach 25 GB/s, while archiving rate is about 1 GB/s. Therefore online processing is advisable to select relevant events and to compress data without loosing their physics content. The overall physics requirements of the HLT are the following:

- **Trigger** Accept or reject events based on detailed online analysis
- **Select** Select a physics region of interest within the event by performing only a partial readout

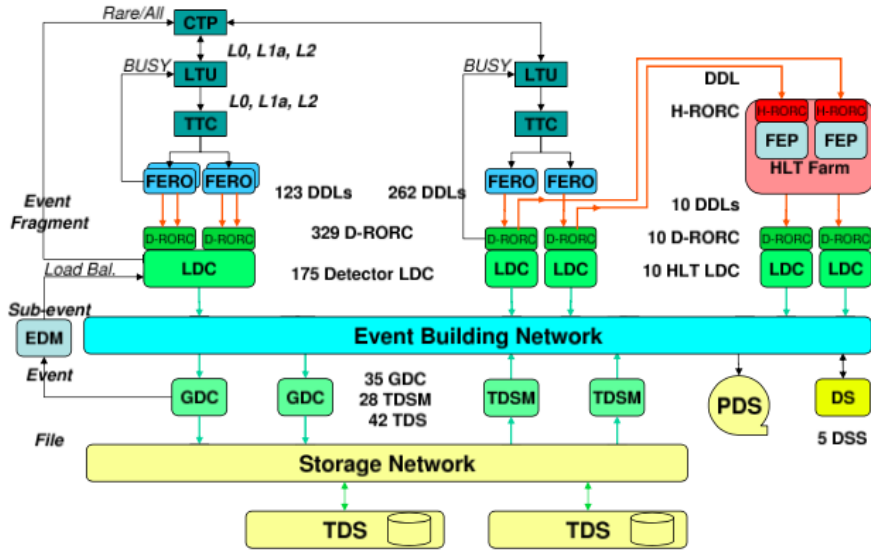


Figure 9: The overall architecture of the ALICE DAQ system and the interface to the HLT system

- **Compress** Reduce the event size without loss of physics information by applying compression algorithms on the accepted and selected data

### 3.2.6 Data flow: from the Online to the Offline

Several stages of processing of raw data taken by detectors before it is available in form of reconstructed events is depicted in Figure 10.

Data originating from the detectors (denoted by 1 in Figure 9) is processed by LDCs and global events are built by GDCs (2), as already mentioned. The so-called publish agent registers the assembled events into the AliEn system (3) and ships them to the CERN computing centre where they are stored first on disks (4) and then permanently on tapes (5) by the CASTOR system.

During data-taking the detectors also produce conditions data that are relevant for the calibration of individual detector signals. Conditions data provide information about the detector status and environmental variables during data-taking. Examples are inactive and noisy channel maps, distributions that describe the response of a channel, temperatures and pressure in a detector, and detector configuration. Many of the conditions data could in principle be calculated from the raw data and extracted offline after data-taking. However, such an

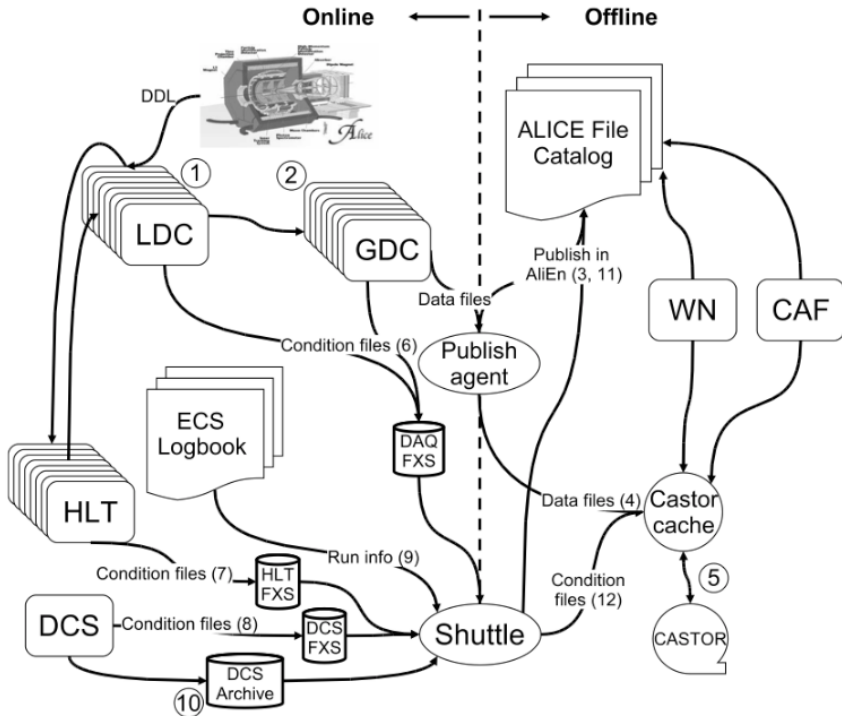


Figure 10: Global view of ALICE's data flow

approach would require an additional pass over the raw data before the reconstruction which is not feasible due to the limited computing resources. Therefore, conditions data are already extracted during data-taking and stored in the Offline Condition Data Base (OCDB). A dedicated program called Shuttle collects these outputs and makes them available to the reconstruction. Furthermore, it retrieves information about the run from the ECS<sup>5</sup> logbook (9) and collects continuously monitored values that are written by DCS into the DCS Archive (10). After processing the data, the Shuttle registers the produced condition files in AliEn (11) and stores the data in CASTOR (12).

With the registration of the raw and conditions data the transition from the online to the offline world has taken place. "Online" denotes all actions and pro-

<sup>5</sup> The Experiment Control System (ECS) is the top level control of the ALICE experiment. Running an experiment implies performing a set of activities on the online systems that control the operation of the detectors. These online systems are: the Trigger (TRG), the Detector Control Systems (DCS), the Data-Acquisition System (DAQ) and the High-Level Trigger (HLT). The ECS provides a framework in which the operator can have a unified view of all the online systems and perform operations on the experiment seen as a set of detectors.

grams that have to run in real time. "Offline" processing is the subsequent step, like for instance the event reconstruction, which is executed on worker nodes (WN) of Grid sites located around the Globe.

### 3.2.7 ALICE Offline software framework

The required computing resources for the reconstruction and analysis of the raw data, as well as the production of simulated events needed for the understanding of the data, exceed the computing power of single institutes and even centres like CERN. Therefore, institutes that are part of the Collaboration provide storage and computing resources. Distribution of the data for reconstruction and analysis cannot be performed manually leading to the need for an automated system. The concept of a decentralised computing model called Grid was identified as a solution.

#### The AliEn Framework

The Grid unifies the resources of distributed computing centres, in particular computing power and storage, to provide them to users all over the World. It allows computing centres to offer their resources to a wider community, and the local resources to be shared by an entire collaboration.

Software that implements the Grid concept is called Grid middleware. Since 2001 ALICE has developed a Grid middleware called AliEn. An ALICE user employs AliEn to connect to the ALICE Grid which is composed of a combination of general services that are provided by many Grid middleware solutions and ALICE-specific services provided by AliEn. Parts of the ALICE Grid are:

1. a global file catalog that is a directory of files in storage elements distributed over the globe
2. the automatic matching of jobs for execution to a suitable location in one of the connected sites
3. a shell-like user interface and iv) API9 services for the ROOT framework

Currently the ALICE Grid consists of about 80 sites located in 21 countries. Figure 11 shows a map of the ALICE Grid sites.



Figure 11: ALICE Grid sites

### The AliRoot Framework

AliRoot is the offline framework for simulation, alignment, calibration, reconstruction, visualisation, quality assurance, and analysis of experimental and simulated data. It is based on the ROOT framework. Most of the code is written in C++ with some parts in Fortran that are wrapped inside C++ code. Re-usability and modularity are the basic features of the AliRoot framework. Modularity allows parts of the code to be replaced, with minimum or no impact on the rest (for example changing the event generator, the transport Monte Carlo or the reconstruction algorithms) which is achieved by implementing abstract interfaces. In addition codes for each detector subsystem are independent modules with their specific code for simulation and reconstruction, which can be developed concurrently with minimum interference. Re-usability is meant to maintain a maximum amount of backward compatibility as the system evolves.

The central module of the AliRoot framework is STEER (Figure 12) which provides several common functions such as steering of program execution for simulation, reconstruction and analysis; general run management; creation and destruction of data structures; initialisation and termination of program phases; base classes for simulation, event generation, reconstruction, detectors elements. For event simulation the framework provides the following functionality:

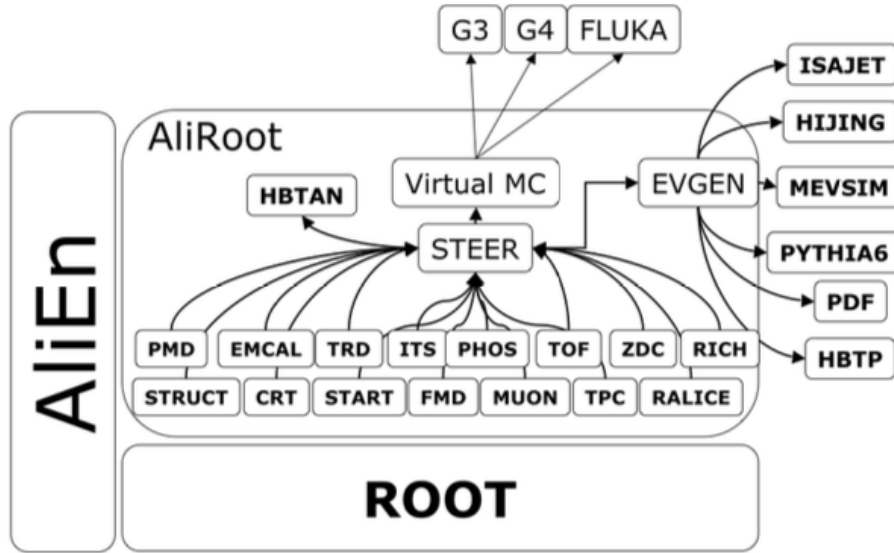


Figure 12: Schema of the AliRoot framework

- **Event Generation:** Many MC event generators (e.g. Pythia, Phojet, EPOS for pp events and HIJING for Pb-Pb events) are interfaced with AliRoot. For each generated particle a list of information (such as type, momentum, charge, production process, originating particle and decay products) is stored in a file (kinematics tree).
- **Transport:** The detector structure, the motion of the particles through it and the possible interactions with the material are simulated using programs such as Geant3, Geant4 and Fluka. For all the interactions of particles with sensitive parts of the detector (hits), information such as position, time, energy deposition and the tag of track they belong to, are recorded during this process
- **Digitisation:** Finally all the hits are translated in the corresponding digital output of the detector, taking into account the detector's response function. All this information are then stored in the specific hardware format of the detector (raw data).

### 3.2.8 Event reconstruction

At this stage the raw data correspond to the signals that would have been produced by an interaction of the same kind within the detector. The subsequent reconstruction is identical, both for simulated as well as real events. It consists of the following steps:

- **Cluster Finding:** Usually, particles that interact with a detector, depending on its spatial segmentation, leave a signal in several adjacent detecting elements. Similarly a signal, last in a time interval can be distributed on more than one time bin. The first required step in the event reconstruction is the cluster finding, i.e the construction of sets of spatial or time close signals that reduce the effect of random noise in the position or timing measurement.
- **Track Reconstruction:** The tracking is a complex and iterative procedure that, starting from clusters, uses the Kalman filter technique to follow inward and outward the track fitting. The tracking is a global task as well as a set of detector-specific procedures. The different steps of the global track reconstruction are schematically reported in Figure 13. The procedure starts from track "seeds" in the outermost part of the TPC, which are selected under the assumption that the corresponding track originated from the primary vertex. Then the TPC only reconstruction ends with a similar seeding in the innermost part of the TPC, the removal of all the clusters already associated to tracks and the final filtering which is performed without requiring that the seeds point to the primary vertex. Subsequently, these tracks are complemented with information from the ITS, TRD, and TOF as well as HMPID and PHOS if the track is in their acceptance, which produces so called "global tracks". Tracks can also be formed out of information from the ITS only.
- **Primary Vertex Reconstruction:** The position of the primary vertex of the interaction can be found using different method based on the usage of different informations such as tracklets in the SPD, tracks in the TPC and global tracks. The estimated position of the primary vertex in each technique is than used to constrain the tracks during the corresponding reconstruction procedure. Of course this constraint is only used for tracks that actually pass in vicinity of the vertex.
- **Secondary Vertex Reconstruction:** The other tracks, sufficiently far away from the primary vertex, are combined to find secondary vertices, corre-

sponding to the decays of unstable particles like the heavy flavour mesons. Such a reconstruction is based on geometrical selection, suggested by the topology of the decay of the considered particles.

The output of the reconstruction is called Event-Summary Data (ESD). This file contains only high-level information such as the position of the event vertex, parameters of reconstructed charged particles together with their PID information, positions of secondary-vertex candidates, parameters of particles reconstructed in the calorimeters and integrated signals of some detectors. This data is further reduced to Analysis-Object Data (AOD) format. These smaller-sized objects contain only information needed for the analysis. Therefore, the transformation procedure may already contain a part of the analysis algorithm, like track selection. Several AODs, focusing on different physics studies, can be created for a given event.

### 3.2.9 Particle identification with the TPC

One of the main characteristics of the ALICE detector, are PID capabilities at a very low transverse momentum threshold of detection. The identification can be performed in two different ways: by direct identification and by the reconstruction of the topology of the disintegration process of a particle.

Particles that live long enough to be identified at track level:  $e^\pm$ ,  $\mu^\pm$ ,  $\pi^\pm$ ,  $K^\pm$ ,  $p^\pm$ , are identified directly. Eight of the detectors that compose ALICE (SDD, SSD, TPC, TRD, TOF, HMPID and the EMCal, DCal) can provide PID, based on different techniques: specific energy loss ( $dE/dx$ ), time of flight and photon radiation characteristics. This information can be used individually or combined.

A second way to identify particles is via invariant mass computation for its daughter particles, as for instance in the case of a strong decay of a resonance, or a weakly decayed particle. In this latter case, reconstruction can be performed via topological reconstruction, since the tracks originate from a decay point that is not the primary interaction vertex. In this second case the direct identification of the daughter particles has an important role in the background reduction.

The TPC provides Particle IDentification (PID) for charged tracks. The gas in the detector is ionised by charged particle traveling through the chamber. In order to identify a particle, the physics observable which is required is energy loss per unit length within the matter crossed by the charged particle. This

specific energy loss denoted by  $dE/dx$ , is described by Bethe-Bloch parameterisation (see Equation 1) that highlights the key of the identification technique. The  $dE/dx$  depends on the charge and the velocity ( $\beta$ ) of the particle, which, in turn, depends only on the momentum and the mass of the ionising particle. Since momentum is already known from the track curvature and the charge is unitary for most measured tracks, measuring the  $dE/dx$  allows us to determine mass indirectly and thus determine the particle species. The following Bethe-Bloch parameterisation gives the mean specific energy loss:

$$-\left\langle \frac{dE}{dx} \right\rangle = k_1 \cdot z^2 \frac{Z}{A} \cdot \frac{1}{\beta^2} \left[ \frac{1}{2} \ln(k_2 \cdot m_e c^2 \cdot \beta^2 \gamma^2) - \beta^2 + k_3 \right] \quad (1)$$

where  $\beta\gamma = p/Mc$  and

Z: atomic number of the ionised gas (in this case Ar/CO<sub>2</sub>/N<sub>2</sub>)

A: mass number of the ionised gas (g/mol)

$m_e$ : electron mass

z: electric charge of the ionising particle in unit of electron charge e

M: ionising particle mass

p: ionising particle momentum

$\beta$ : ionising particle velocity normalised to the light velocity c

$\gamma = 1/\sqrt{1 - \beta^2}$ , Lorentz factor

$k_1, k_2, k_3$ : constants depending on the ionised medium

The specific energy loss in the TPC as a function of momentum is shown in Figure 7. The different bands show expected values for  $e^\pm$ ,  $\pi^\pm$ ,  $K^\pm$ ,  $p^\pm$  and deuteron. These correspond to the statistical distribution of the measured energy loss.

The expected value which corresponds to the prediction by the Bethe-Bloch parameterisation is shown as black lines on Figure 6. For a track within the TPC, the relevant quantity to be considered for PID is the difference between the specific energy loss measured by the detector and the corresponding value predicted by the Bethe-Bloch parametrisation. The difference could be expressed in a number of  $\sigma$  as shown in Equation 2. In this way, it is possible to estimate the goodness of a mass hypothesis more quantitatively. It also provides the possibility to choose strictness to be adopted for the identification by applying a different value of  $n_\sigma$ .

$$n_\sigma = \frac{(dE/dx)_{\text{measured}} - (dE/dx)_{\text{Bethe-Bloch}}}{\sigma_{\text{TPC}}} \quad (2)$$

### 3.2.10 Centrality Determination?

Depends if we do the PbPb analysis or the high multiplicity analysis for the  $K^{*\pm}$

### 3.2.11 ITS UPGRADE?

OPTIONAL

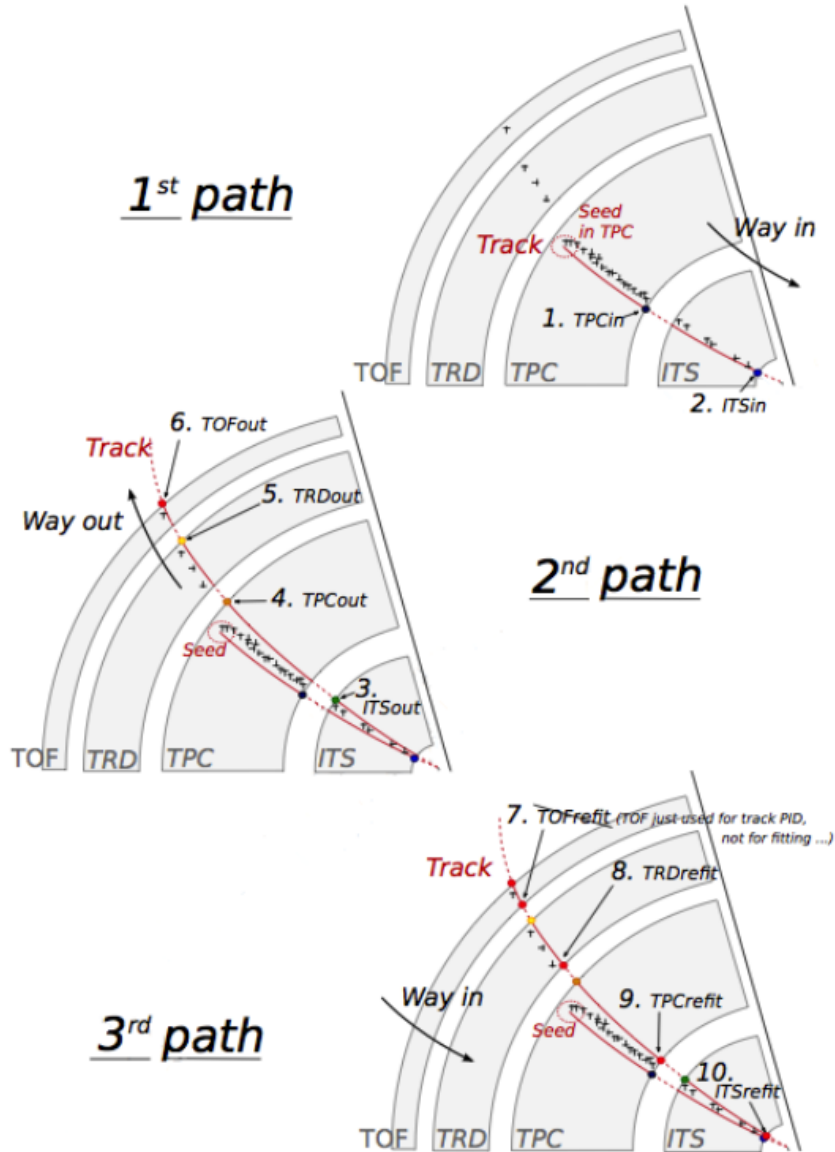


Figure 13: Principle of track reconstruction in an ALICE event: all the three steps of the iterative procedure are shown. The numbers on the plots marks the bits that are activated in each step during the Kalman filter procedure, in case of success

# 4 | $K^{*0}$ AND $K^{*\pm}$ RESONANCE RECONSTRUCTION IN PP COLLISIONS

Short lived resonances are good probes to study the properties of strongly interacting matter produced in high energy heavy ion collisions.

## 4.1 Signal Extraction

We describe how hadronic resonances are usually reconstructed from the raw data

### 4.1.1 Uncorrelated background estimate

Description of event mixing, like-sign and rotating background

## 4.2 $K^{*\pm}$ Mass Determination

$K^{*\pm}$  mass has been extracted using the following procedure.

### 4.2.1 Systematic uncertainty on mass estimation

# 5

## MEASUREMENT OF $K^{*\pm}$ PRODUCTION IN PP COLLISIONS

$K^{*\pm}$  is a resonance particle with a small lifetime ( $\sim 4 \text{ fm}/c$ ), comparable to that of the fireball which is produced during the heavy ion collision. Due to its short lifetime, it can be used to study the re-scattering and regeneration effects.  $K^{*\pm}$  can provide the information regarding strangeness enhancement as it contains a strange quark. Measurements of  $K^{*\pm}$  in pp collisions can be used as a baseline to study the PbPb collisions at the LHC energy and to provide a reference for tuning event generators.

### 5.1 $K^{*\pm}$ reconstruction in pp collisions

General idea behind the reconstruction procedure

#### 5.1.1 Data sample and event selection

Details of the data used and event selection criteria applied

#### 5.1.2 Primary pion selection

Selection cuts applied to the primary pion daughters of  $K^{*\pm}$

#### 5.1.3 $V^0$ selection

Selection criteria for  $K_S^0$

#### 5.1.4 Signal Extraction

Signal extraction procedure including estimation of background and normalisation

#### 5.1.5 Raw Yield Estimation

Fitting procedure and fit function details

### **5.2 Efficiency Correction**

We use Monte Carlo to estimate the detector acceptance x efficiency

### **5.3 Systematic Uncertainties estimation**

Estimation of systematic uncertainties

### **5.4 $K^{*\pm}$ transverse momentum spectrum**

Final  $p_T$ spectra obtained

# 6 | $K^0$ COMPARISONS

## **6.1 $K^0$ reconstruction in pp collisions**

We define the details of reconstruction of  $K^0$  in pp collisions

## **6.2 Comparison of $K^0$ and $K^{*\pm}$**

Comparison of  $K^{*0}$  and  $K^{*\pm}$  spectra and efficiencies

# 7 | FURTHER RESULTS AND DISCUSSIONS

## 7.1 Particle Ratios

$K^{*\pm} / K^0$  ratios in different system sizes

## 7.2 Model Comparison

Comparison with different theoretical models

## 7.3 Energy Dependence

Energy dependence study for  $K^{*\pm}$

## 7.4 $K^{*+}$ vs $K^{*-}$

Study of particle vs anti-particle from data and monte carlo

## CONCLUSIONS